Relating individual characteristics to resting state fMRI networks

John Cocjin (cocjinjb)[1], Jonathan Fisher (jofisher)[1], Charles Chen[2]
[1]CS224W, [2]CS229

1. Introduction

Resting-state functional MRI (rsfMRI) measures the brain's intrinsic activity - i.e. the dynamics of the brain when a person is relatively unengaged. In the course of an rsfMRI scan, a subject is imaged in the MRI scanner while they are 'not really doing much'; e.g., attending only to a cross on a screen.

In conventional analyses of rsfMRI, we look at the relations between the time series of different brain regions, asking: what regions fluctuate together? These regions are thought of as connected in some fundamental way relating not to the context (task) that a subject is in but rather their underlying physiology and individual traits (Mathews 2016). For example, nodes of the traditional sensorimotor network, implicated in sensation and motor action, actively coexpress within rsfMRI measurements. They further vary in their within-network connectivity from subjects with or without Parkinson's, a form of motor impairment (Tahmasian 2015).

Herein, we take advantage of the Human Connectome Project (HCP) study, which includes rsfMRI and behavioral, cognitive, and demographic metrics from 1003 healthy adult subjects. With this dataset, unprecedented in its scale, we ask: how do the interactions of resting state subnetworks relate to subject wise measures? Specifically, in this project, we investigate the the relation of network metrics on rsfMRI graphs to to subject-wise non-imaging variables.

2. Related Work

2.1. Predicting with rsfMRI

Because of the simplicity in its acquisition, rsfMRI has been collected on and compared among a wide array of individuals, ranging from healthy adult subjects, like those of the HCP study, to subjects with neurological/cognitive conditions such as schizophrenia, Parkinson's, and ADHD (Bassett 2011, Tahmasian 2015, Rosenberg 2016). These studies attempt to explain population differences via rsfMRI features, often an ensemble of temporal correlations (edges) among relevant brain regions (nodes). While a few recent examinations have differentiated their conditions of interest with high reliability, the majority have not (Shen 2017). As a result, claims on the fundamental mechanisms underlying cognitive or neurological differences are only weakly interpretable. Many of these studies are firstly plagued by low subject counts, despite being considered high (order of tens) in conventional neuroscientific standards. Recent efforts such as the Human Connectome Project are keenly aware of these difficulties and have begun collecting fMRI (including rsfMRI) imaging and behavioral sets on an unprecedented scale, on the order of hundreds to thousands of subjects. Here, we examine the HCP dataset, for which few studies have been conducted in relating the panoply of available subject-wise measures collected to derived rsfMRI metrics (Smith 2015, Hearne 2016).

2.2. Network metrics

The studies that we identified as investigating subject variables on HCP have primarily taken as features the region-to-region temporal correlations. They examine: 'how does this region-to-region connectivity (correlation) covary with a given subject measure?' Region-to-region measures lend themselves to simple interpretations, ex. that the stereotyped covariation of the motor cortex and the basal ganglia may be implicated in motor skill differences. However, they fail to capture network wide phenomena relating to brain wide coordination (clustering, allegiance, etc.). Network wide phenomena have indeed been implicated, albeit weakly, in behavioral and cognitive differences (Wang 2010, Bassett 2017). For example, subjects with schizophrenia have been identified as differing from healthy controls in resting state network metrics of 'strength' and 'diversity' (Bassett 2011). While this early exploration on schizophrenia remains conservative on cognitive interpretation of the metrics, rather focusing on population discriminability, other

work has been completed in constructing salient network measures. It is possible to construct hypotheses, e.g. the 'flexibility' of networks in their connections may or may not contribute to cognitive capacity (Bassett 2017). We thus adapt metrics from network science in our examination of the HCP dataset.

3. Methods

3.1. Imaging and behavioral data

We examine resting state fMRI (rsfMRI) and non-imaging data of 1003 healthy adults who participated in the Human Connectome Project (Van Essen 2013). Each subject underwent two 15-minute rsfMRI scans in two separate sessions for a total of one hour of resting-state data. In the resting-state paradigm, subjects are instructed to fixate on a cross hair displayed on a screen while in the MRI scanner for the duration of the scan. Each resting state scan was collected at 3T via slice-accelerated echo-planar imaging at a spatial resolution of 2 mm isotropic and a temporal resolution of 0.7 s.

The collected non-imaging data includes demographic and family history information as well as scoring in a suite of cognitive/behavioral testing (Van Essen 2013). We are necessarily restricted to the subset of measures that are specified as accessible to the general public. For this milestone, we choose measures that belong to the following categories of measurement: Alertness, Cognition, Emotion, Motor, Personality, and Sensory. This resulted in 177 different subject wise measures. Categorical measures are encoded on a numerical scale, and all measures are normalised. We list several examples of the subject wise measures in Table 1, along with their categories and assessment subcategories.

Table 1. Examples of subject wise measures with their assessment types, categories, and descriptions.

Shorthand	Assessment Type	Category	Description
PSQI_Score	Sleep	Alertness	Sleep (Pittsburgh Sleep Questionnaire) Total Score
PMAT24_A_CR	Fluid Intelligence	Cognition	Penn Matrix Test: Number of correct responses
AngAffect	Negative Affect	Emotion	NIH Toolbox: Anger-Affect Survey
Dexterity	Dexterity (9-hole Pegboard)	Motor	NIH Toolbox 9-hole Pegboard Dexterity Test
Strength_AgeAdj	Strength	Motor	NIH Toolbox Grip Strength Test: Age adjusted score

3.2. Image preprocessing

The raw fMRI signal was preprocessed to remove functional signal confounds such as head motion . All subjects' image sets were further aligned to the MSM anatomical template to establish spatial anatomical correspondence. In this manner, we may compare similar spatial regions across subjects (e.g. we then know where the motor cortex of both subject 1 and 2 exist based on anatomy). The preprocessing workflow is fully described in Glasser 2013, Salimi-Khorshidi 2014, and Robinson 2014.

3.3 Dimensionality reduction on the behavioral measures

All subject wise measures are normalised and then input into principal components analysis to reduce the dimensionality of the measures. The principal component with the largest eigenvalue (PC1) is used to sparsify network edges, as will be explained later. It is also taken as a summary for the subject-wise measures. We project each subjects' full measures onto PC1 to extract subject-wise PC1 scores. We correlate PC1 with each measure to investigate which measures are captured by PC1; the cumulative distributions of correlations by category of measure are shown in the following figure. As can be seen, PC1 correlates most with the measures from the emotion and personality categories. We may also examine the top 7 measures that correlate with PC1, as shown in table 2.

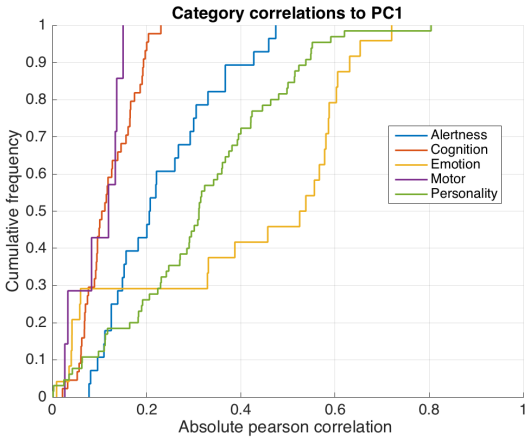

Figure 1. Cumulative histogram of correlations between measures within given category to PC1.

Table 2. Top 7 subject measures for correlation with PC1, reporting correlation, categories, and description.

Shorthand	Correlation	Category	Description
NEOFAC_N	0.804	Personality	NEO-FFI Neuroticism (NEOFAC_N)
PercStress	0.720	Emotion	NIH Toolbox Perceived Stress Survey Score
Loneliness	0.653	Emotion	NIH Toolbox Loneliness Survey Score
Sadness	0.631	Emotion	NIH Toolbox Sadness Survey Score
NEORAW_26	0.620	Personality	Scale report: Sometimes I feel completely worthless
AngHostil	0.606	Emotion	NIH Toolbox Anger-Hostility Survey Score
LifeSatisf	-0.603	Emotion	'NIH Toolbox General Life Satisfaction Survey Score

Due to computational limitations in using PC1 for network sparsification, we do not consider other PCs.

3.4. Network construction

Undirected, weighted graphs for fMRI, referred to as functional connectivity matrices, are computed per subject as follows:

Nodes:

Group spatial ICA was applied to the preprocessed rsfMRI data (Smith 2014a, FastICA/MELODIC). All subject's image sets (space (x,y,z) by time (t)) are concatenated relative to time, and an approximation of spatial PCA is performed. ICA is performed on the PCA spatial matrix to provide our nodes - 300 spatial ICA maps that represent regions that tend to co-activate. Several ICs and their time courses are provided in [figure 1]. The IC maps (nodes) are propagated back to each subject, and the original subject-wise spatiotemporal data is projected onto the ICs in order to extract the node time series per subject per IC node.

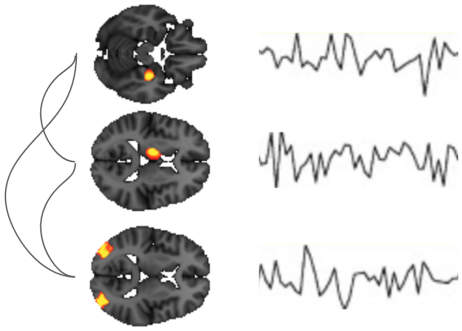

Figure 2. 3/300 independent components (nodes), their time series, and edges.

Edges:

Edges are taken as the absolute value of partial correlation between node time series with L2 tikhonov regularisation (FSLNets, rho = 0.01) (Smith et al 2011). Partial correlation refers to the Fisher transformed correlation between two time series adjusted after regressing out the time series of unconsidered network nodes, attempting to remove the influences of indirect network connections. Our edges therefore measure the extent to which distinct spatial maps directly covary over time. We further scale our edge values to lie within [0, 1], normalised by the largest edge value across subjects.

Full vs. strong networks

For the upcoming analyses, we examine 4 versions of our network. We first consider the full weighted network. Given that some weighted edges may be uninformative to the prediction task, and so may introduce noise into network feature calculations, we mask edges out of the network. To construct this mask, we calculate the correlation of each edge weight to the PC1 subject measure. In this manner, we extract which edges more strongly correlate to PC1. We create masks thresholded for the 75th, 85th, and 95th percentiles of the absolute value of the correlation. This procedure provides us with 4 networks, that we denote as 75, 85, 95, and full. Each of these networks have 22500, 13500, 4500, and 90000 nonzero edges respectively.

3.4. Network features

We consider 23 weighted network metrics. For non-scalar metrics (node-by-node or edge-by-edge), we extract the mean, standard deviation, and max. Features may be computed on absolute values of the edge weights; this is designated by "on absolute." Features may be computed on the positive or negative edge subset of the network as designated by "positive or negative signed". Features are listed in table 3.

Table 3. Network features considered.

Strength on absolute	Negative signed strength	Positive signed strength	Clustering coefficient on absolute
Positive signed clustering coeff	Negative signed clustering coeff	Transitivity on absolute	Efficiency on absolute
Modularity on absolute	Modularity	Assortativity on absolute	Core periphery
Core periphery	Weighted distance	Number edges in distance matrix	Mean first passage on absolute
Diffusion efficiency	Node betweenness on absolute	Edge betweenness on absolute	Eigenvector centrality on absolute
Eigenvector centrality	Pagerank centrality on absolute	Pagerank centrality	

For a subset of features that are found as relevant in analyses, we list their equations, for reference. Further details on formulation may be found in Rubinov 2010.

- **Distance:** distance_wei(L)
  The input matrix must be a mapping from weight to distance (weight inversion $l_{i,j} = \frac{1}{|w_{i,j}|}$).
  Here we measure the shortest weighted distance between every 2 nodes and the number of edges in this shortest path.

$$d_{i,j} = min\{l_{i\to j}\}$$

$$b_{i,j} = \#egdes(d_{i,j})$$

  Where $min\{l_{i\to j}\}$ is the minimum of all sums of weighted distances for all paths that connect i and j and $\#egdes(d_{i,j})$ is the number of edges in $d_{i,j}$

  The features that we used are the mean, standard deviation and maximum of the $d_{i,j}$ and $b_{i,j}$ calculated over the network.

- **Diffusion efficiency:** diffusion_efficiency($|WU|$)
  The diffusion efficiency between nodes i and j is the inverse of the mean first passage time from i to j, that is the expected number of steps it takes a random walker starting at node i to arrive for the first time at node j.
  The features that we used are the mean, standard deviation and maximum of the diffusion efficiency calculated over the network absolute value.

- **Weighted Clustering coefficient:** clustering_coef_wu($|WU|$), clustering_coef_wu_sign(WU)
  The clustering coefficient is the fraction of triangles around a node and is equivalent to the fraction of nodes neighbors that are neighbors of each other.
  The weighted clustering coefficient is similar,

$$c_i = \frac{t_i^w}{k_i(k_i - 1)}$$

  where k_i is the number of node i neighbors and t_i^w is the sum of "weighted triangles" that includes node i. A weighted triangle is the third root of the three edges product $(w_{ij}w_{ik}w_{jk})^{\frac{1}{3}}$.

  The features that we used are the mean, standard deviation and maximum of the weighted Clustering coefficient calculated over the network absolute values, only positive edges and only negative edges in a given network.

- **Strength:** strengths_und($|WU|$), strengths_und_sign(WU)
  Node strength is the sum of weights of links connected to the node.

$$s_i = \sum_{j \neq i} w_{ij}$$

The features that we used are the mean, standard deviation and maximum of the strength calculated over the network absolute values, only positive edges and only negative edges in a given network.

3.5. Univariate evaluation

We characterize how well a given input (edge or network feature) relates to PC1 with the pearson correlation. Pearson correlation measures the strength of linear association between two variables. The pearson correlations from edges, and then features extracted from the 4 defined networks, to PC1 are examined. From this, we may examine (1) are raw edge weights more or less informative than features computed on the full network?, and (2) are features computed on the thresholded networks more or less informative than raw edge weights or features from the full network?

3.6. Multivariate evaluation

We investigate whether multivariate regression considering all extracted network features can predict PC1 and subject-wise variables from our four networks. We first explore among 10 kinds of regression models (see Table 3) to see which best predicts PC1. We characterize fitting performance by MSE of prediction on the testing set. We separate our data from 1003 samples into two parts: training set with 903 samples, and test set with 100 samples. As the behavioral metrics are all normalized, the smaller MSE is, the better a model is fitting.

As seen, across the network with top 15% most correlated edges with PC1, generalized linear model with all quadratic terms significantly outperforms others. We therefore use this regression method for multivariate prediction of all 177 subject-wise variables. Not hard to imagine, there are behavioral metrics which are intrinsically not very predictable (and that is why we use PC1 to evaluate different models). Therefore, we would report the top 5 predictable (in sense of MSE on the test set) for each network, as well as their MSEs. Generalized linear model (GLM) is a regression model that gives the probability of predicted y by a distribution from the exponential family:

$$p(y;\eta) = b(y)\exp(\eta^T T(y) - a(\eta))$$

where η is the canonical parameter given by $\eta(x)$. Here, GLM with quadratic terms computes the canonical parameter with weighted sum of all 1st and 2nd order terms from x:

$$\eta(x) = \begin{bmatrix} x^\intercal & 1 \end{bmatrix} \boldsymbol{W} \begin{bmatrix} x \\ 1 \end{bmatrix}.$$

Table 4. Regression/classification algorithms attempted.

Model	PC1 Test Set Prediction MSE
Multivariate linear regression	0.8688
Generalized Linear Model with quadratic terms	0.1357
Support vector machine regression with linear kernel	4.9087
Support vector machine regression with 2nd order polynomial kernel	1 (not converge)
Support vector machine regression with 3nd order polynomial kernel	1 (not converge)
Support vector machine regression with 4nd order polynomial kernel	1 (not converge)
Support vector machine regression with gaussian kernel (FWHH radius = 100)	0.9907
Support vector machine regression with gaussian kernel (FWHH radius = 10)	0.8474
Support vector machine regression with gaussian kernel (FWHH radius = 1)	0.7985
Support vector machine regression with gaussian kernel (FWHH radius = 0.1)	0.8298

4. Results & Discussion

4.1 Edge weights exist that correlate more strongly with PC1 than full network features.

We first compare whether edge weights or full network features more strongly correlate with PC1. As can be seen in figure 3, while the full network features (median correlation = 0.0479) are usually more informative than those of the edges (median correlation = 0.0229), there do exist edges with higher correlations than the maximum of the full network features (max for full: 0.0887, edges: 0.1552). We visualize the top 5 edges in figure 4.

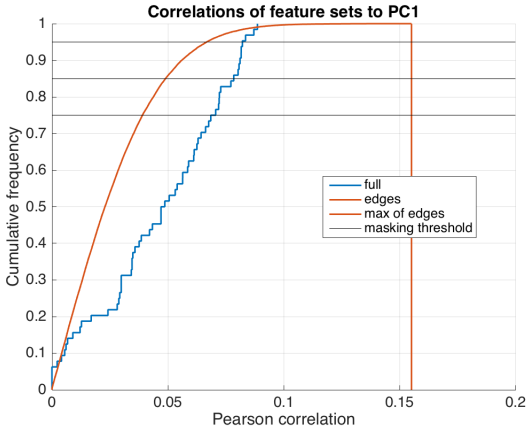

Figure 3. Cumulative histogram of absolute pearson correlations of either edge weights or full network features.

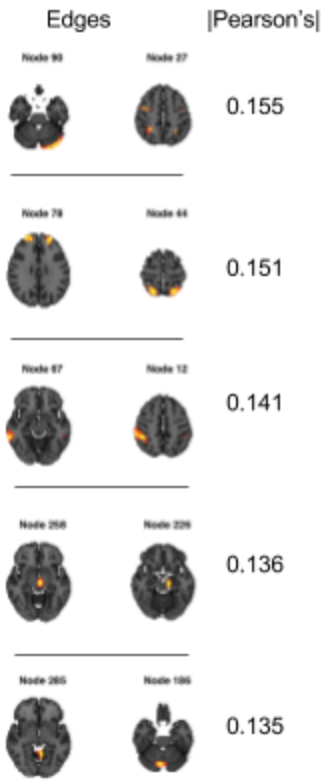

Figure 4. Strongest edges with their pearson's correlation and associated nodes.

4.2. Strong network features correlate more strongly with PC1 than strong edges.

We sought to investigate whether these 'strong' edges formed subnetworks with more informative network features. To create strong networks, we thresholded out edges that lie below the 75th, 85th, and 95th percentiles of the edge distribution, as seen in Fig 1. We compare whether edge weights or strong network features more strongly correlate with PC1. As can be see in figure 5 and table 5, the strong networks have features with a higher maximum correlation than that of the raw edge weights. This suggests that the strong edge subnetworks indeed provide additional information at the global level.

Table 5. Summary measures on correlations to PC1 within a given feature set.

Feature set	Mean	Median	Maximum
Edges	0.0271	0.0229	0.1552
Full network	0.0463	0.0479	0.0887
75 network	0.0697	0.0692	0.183
85 network	0.0804	0.0874	0.192
95 network	0.0661	0.0558	0.164

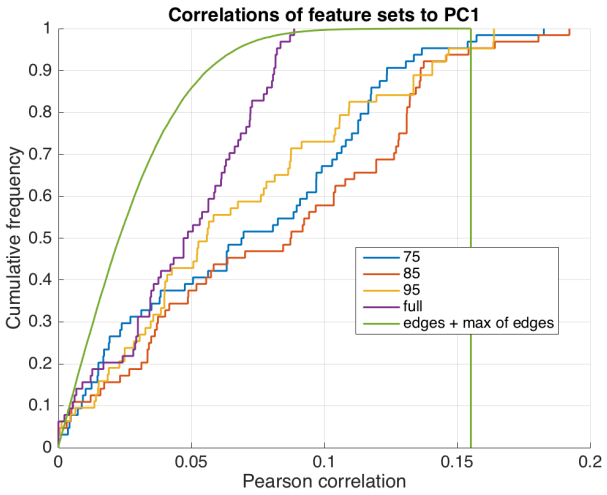

Figure 5. Cumulative histogram of absolute pearson correlations of either edge weights or network features. As can be seen, 'strong' networks yield informative global network features.

4.3. Strong networks with different thresholds accentuate different correlative features

The 5 most correlated features for each network are shown in table 6. Among the top 10 most correlated features for each network, strikingly, only one variable is shared: mean diffusion efficiency. This suggests that the masking threshold yields subnetworks with differentially relevant global features.

Table 6. Global network features that most correlate with PC1 within network, rank ordered.

75		85		95	
Variable	Pearson's	Variable	Pearson's	Variable	Pearson's
Std of negative signed clustering coefficient	-0.183	Mean diffusion efficiency	-0.192	Efficiency	-0.16385
Max negative signed clustering coefficient	-0.157	Std of distance	0.181	Mean diffusion efficiency	-0.1636
Max strength on absolute	-0.154	Std of negative signed clustering coefficient	-0.16416	Mean core periphery on absolute	-0.14682
Mean diffusion efficiency	-0.137	Mean of distance	0.15428	Std of core periphery on absolute	-0.14569
Std of distance	0.134	Mean of negative signed clustering coefficient	-0.1459	Assortativity	0.14065

4.4. Multivariate prediction for subject measures improves in using strong networks.

We were interested in whether the introduction of strong network extraction improved test set validation MSE. As seen in figure 6, a GLM predictor trained on strong network features has a large decrease in MSE relative to the full network features for the majority of features.

We further examine the top 5 individual measures predicted in the multivariate procedure from each network. Categories and correlations to PC1 of these measures are listed in table 8. It's striking in that the measures best predicted by the strong networks constructed are not necessarily of the Emotion or Personality Category and may, in fact, have low correlation to PC1.

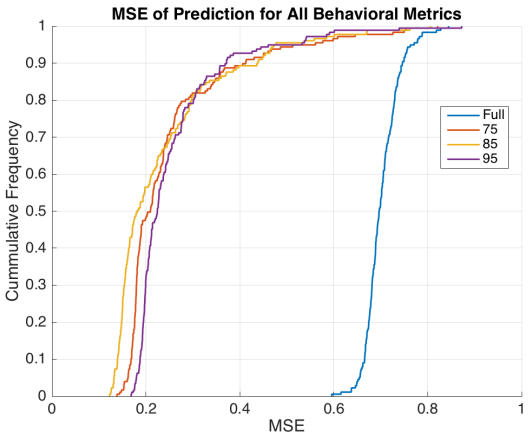

Figure 6. Cumulative histogram of mean squared error of prediction for all measures using our four networks.

Table 7. Top 5 measures predicted by multivariate prediction from each network.

MSE reported	Full	75	85	95
PC1	0.649	0.1694	0.1357	0.2146
1st_Best_Predicted_Metric	Strength_AgeAdj	NEORAW_03	NEOFAC_A	Mars_Final
	0.5956	0.1383	0.1226	0.1686
2nd_Best_Predicted_Metric	Strength_Unadj	Mars_Log_Score	NEORAW_08	Mars_Log_Score
	0.6153	0.1444	0.125	0.1697
3rd_Predicted_Metric	IWRD_RTC	Mars_Final	NEORAW_37	Noise_Comp
	0.6373	0.148	0.1259	0.1736
4th_Best_Predicted_Metric	Noise_Comp	ListSort_Unadj	Odor_Unadj	ReadEng_AgeAdj
	0.6377	0.1527	0.1264	0.1757
5th_Best_Predicted_Metric	PSQI_Score	GaitSpeed_Comp	Odor_AgeAdj	DDisc_SV_3yr_200
	0.6461	0.153	0.1302	0.1761

Table 8. Measures best predicted by strong network features listed with category and correlation to PC1.

DDisc_SV_3yr_200: Cognition: -0.156	GaitSpeed_Comp: Motor: -0.083	ReadEng_AgeAdj: Cognition: -0.101
ListSort_Unadj: Cognition: -0.112	Mars_Final: Sensory: 0.040	Mars_Log_Score: Sensory: 0.040
NEOFAC_A: Personality: -0.515	NEORAW_03: Personality: -0.112	NEORAW_08: Personality: -0.113
NEORAW_37: Personality: -0.424	Noise_Comp: Sensory: 0.053	Odor_AgeAdj: Sensory: -0.015
Odor_Unadj: Sensory: -0.011		

5. Conclusions and future directions

We explored how global features of resting state brain networks may be informative towards distinguishing behavioral measures of individuals. We see that network edge weights can correlate more highly with a latent measure (PC1) than global features of the fully connected network. We find that the subnetworks formed from these highly correlative edges yield global network properties that are further relevant towards the latent measure. Additionally, in the framework of multivariate regression, we can better predict the majority of individual behavioral measures with global features from the strong network than global features from the full network, despite having low correlation with our PC1. The behavioral measures that can be predicted correlate highly with the extracted latent measure (PC1). Here, PC1 correlates strongly with a subset of personality and emotion measurements.

Unfortunately, we were unable to run this set of analysis on further PCs due to computational limitations. We anticipate that further PCs would capture other underlying behavioral factors (quite possibly intelligence, motor control, etc.). It would be interesting to compare network edges and global properties among the different PCs. It may be the case that certain edges do overlap between the PCs, which may suggest that these edges serve multiple roles in mediating individual factors. It may also be the case that the edges are largely unshared between PCs, possibly indicating segregation of the mediation. We would conjecture, however, that the fact that network properties of the strong networks built from PC1 can improve prediction of measures that do not necessarily correlate with PC1 indicates the former (overlapping roles) more than the latter (strict segregation of mediation).

It is worth mentioning that previous literature has had corresponding difficulty predicting healthy cognitive/behavioral variables from resting state fMRI (Smith 2015, Shen 2015). Certainly, this poor predictive power calls into question strong interpretations on these network metrics (Rubinov 2010). We are hopeful that techniques looking at subnetworks, as opposed to the full network, will increase practical discriminability of behavioral metrics, and enable interpretation of brain activity and translation of prediction techniques to the clinic. One may easily imagine using our interpretations of these network metrics to design interventions that modulate the brain network landscape of a patient, or to detect pathological states reliably among individuals (Bassett 2017, Matthews 2016, Rubinov 2010, Shen 2017).

Contributions:
Jonathan (jofisher) and John (cocjinjb) contributed equally for network metric extraction and univariate analysis for CS224W. Charles, Jonathan, and John wrote our respective portions for our respective courses. Charles did multivariate prediction for CS229.

We would also like to thank Dr. Manish Saggar for discussion and guidance on how to approach this dataset.

References

Bassett, D. S., & Sporns, O. (2017). Network neuroscience. Nature neuroscience, 20(3), 353.

Bassett, D. S., Nelson, B. G., Mueller, B. A., Camchong, J., & Lim, K. O. (2012). Altered resting state complexity in schizophrenia. Neuroimage, 59(3), 2196-2207.

Cole, D. M., Smith, S. M., & Beckmann, C. F. (2010). Advances and pitfalls in the analysis and interpretation of resting-state FMRI data. Frontiers in systems neuroscience, 4.

Cox, R. W. (1996). AFNI: software for analysis and visualization of functional magnetic resonance neuroimages. Computers and Biomedical research, 29(3), 162-173.

Craddock, R. C., Tungaraza, R. L., & Milham, M. P. (2015). Connectomics and new approaches for analyzing human brain functional connectivity. Gigascience, 4(1), 13.

Glasser, M. F., Sotiropoulos, S. N., Wilson, J. A., Coalson, T. S., Fischl, B., Andersson, J. L., ... & Van Essen, D. C. (2013). The minimal preprocessing pipelines for the Human Connectome Project. Neuroimage, 80, 105-124.

Matthews, P. M., & Hampshire, A. (2016). Clinical concepts emerging from fMRI functional connectomics. Neuron, 91(3), 511-528.

Hearne, L. J., Mattingley, J. B., & Cocchi, L. (2016). Functional brain networks related to individual differences in human intelligence at rest. Scientific reports, 6, 32328.

Richiardi, J., Altmann, A., Milazzo, A. C., Chang, C., Chakravarty, M. M., Banaschewski, T., ... & Conrod, P. (2015). Correlated gene expression supports synchronous activity in brain networks. Science, 348(6240), 1241-1244.

Robinson, E. C., Jbabdi, S., Glasser, M. F., Andersson, J., Burgess, G. C., Harms, M. P., ... & Jenkinson, M. (2014). MSM: a new flexible framework for multimodal surface matching. Neuroimage, 100, 414-426.

Rubinov, M., & Sporns, O. (2010). Complex network measures of brain connectivity: uses and interpretations. Neuroimage, 52(3), 1059-1069.

Salimi-Khorshidi, G., Douaud, G., Beckmann, C. F., Glasser, M. F., Griffanti, L., & Smith, S. M. (2014). Automatic denoising of functional MRI data: combining independent component analysis and hierarchical fusion of classifiers. Neuroimage, 90, 449-468.

Shen, X., Finn, E. S., Scheinost, D., Rosenberg, M. D., Chun, M. M., Papademetris, X., & Constable, R. T. (2017). Using connectome-based predictive modeling to predict individual behavior from brain connectivity. nature protocols, 12(3), 506-518.

Smith, S. M., Miller, K. L., Salimi-Khorshidi, G., Webster, M., Beckmann, C. F., Nichols, T. E., ... & Woolrich, M. W. (2011). Network modelling methods for FMRI. Neuroimage, 54(2), 875-891.

Smith, S. M., Hyvärinen, A., Varoquaux, G., Miller, K. L., & Beckmann, C. F. (2014). Group-PCA for very large fMRI datasets. NeuroImage, 101, 738-749.

Tahmasian, M., Bettray, L. M., van Eimeren, T., Drzezga, A., Timmermann, L., Eickhoff, C. R., ... & Eggers, C. (2015). A systematic review on the applications of resting-state fMRI in Parkinson's disease: Does dopamine replacement therapy play a role?. Cortex, 73, 80-105.

Van Essen, D. C., Smith, S. M., Barch, D. M., Behrens, T. E., Yacoub, E., Ugurbil, K., & Wu-Minn HCP Consortium. (2013). The WU-Minn human connectome project: an overview. Neuroimage, 80, 62-79.

Wang, Jinhui, Xinian Zuo, and Yong He. "Graph-based network analysis of resting-state functional MRI." Frontiers in systems neuroscience 4 (2010).

Hearne, Luke J., Jason B. Mattingley, and Luca Cocchi. "Functional brain networks related to individual differences in human intelligence at rest." Scientific reports 6 (2016): 32328.